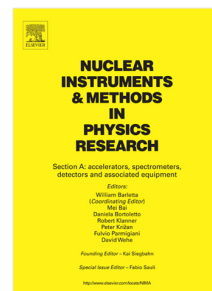


Journal Pre-proof

Progress on the PICOSEC-Micromegas Detector Development: Towards a precise timing, radiation hard, large-scale particle detector with segmented readout

K. Kordas, J. Bortfeldt, F. Brunbauer, C. David, D. Desforge, G. Fanourakis, J. Franchi, M. Gallinaro, F. García, I. Giomataris, D. González-Díaz, T. Gustavsson, C. Guyot, F.J. Iguaz, M. Kebbiri, P. Legou, J. Liu, M. Lupberger, O. Maillard, I. Maniatis, I. Manthos, H. Müller, V. Niaouris, E. Oliveri, T. Papaevangelou, K. Paraschou, M. Pomorski, B. Qi, F. Resnati, L. Ropelewski, D. Sampsonidis, T. Schneider, P. Schwemling, L. Sohl, M. van Stenis, P. Thuiner, Y. Tsipolitis, S.E. Tzamarias, R. Veenhof, X. Wang, S. White, Z. Zhang, Y. Zhou



PII: S0168-9002(19)31298-7
DOI: <https://doi.org/10.1016/j.nima.2019.162877>
Reference: NIMA 162877

To appear in: *Nuclear Inst. and Methods in Physics Research, A*

Received date: 9 April 2019
Revised date: 25 September 2019
Accepted date: 27 September 2019

Please cite this article as: K. Kordas, J. Bortfeldt, F. Brunbauer et al., Progress on the PICOSEC-Micromegas Detector Development: Towards a precise timing, radiation hard, large-scale particle detector with segmented readout, *Nuclear Inst. and Methods in Physics Research, A* (2019), doi: <https://doi.org/10.1016/j.nima.2019.162877>.

This is a PDF file of an article that has undergone enhancements after acceptance, such as the addition of a cover page and metadata, and formatting for readability, but it is not yet the definitive version of record. This version will undergo additional copyediting, typesetting and review before it is published in its final form, but we are providing this version to give early visibility of the article. Please note that, during the production process, errors may be discovered which could affect the content, and all legal disclaimers that apply to the journal pertain.

© 2019 Published by Elsevier B.V.

Progress on the PICOSEC-Micromegas Detector Development: towards a precise timing, radiation hard, large-scale particle detector with segmented readout

K. Kordas^{d,*}, J. Bortfeldt^b, F. Brunbauer^b, C. David^b, D. Desforge^a, G. Fanourakis^e, J. Franchi^b, M. Gallinaro^g, F. García¹, I. Giomataris^a, D. González-Díazⁱ, T. Gustavsson^j, C. Guyot^a, F.J. Iguaz^{a,1}, M. Kebbiri^a, P. Legou^a, J. Liu^c, M. Lupberger^b, O. Maillard^a, I. Maniatis^d, I. Manthos^d, H. Müller^b, V. Niaouris^d, E. Oliveri^b, T. Papaevangelou^a, K. Paraschou^d, M. Pomorski^k, B. Qi^c, F. Resnati^b, L. Ropelewski^b, D. Sampsonidis^d, T. Schneider^b, P. Schwemling^a, L. Sohl^a, M. van Stenis^b, P. Thuiner^b, Y. Tsiopolitis^f, S.E. Tzamarias^d, R. Veenhof^{h,2}, X. Wang^c, S. White^{b,3}, Z. Zhang^c, Y. Zhou^c

^aIRFU, CEA, Université Paris-Saclay, F-91191 Gif-sur-Yvette, France

^bEuropean Organization for Nuclear Research (CERN), CH-1211 Genève 23, Switzerland

^cState Key Laboratory of Particle Detection and Electronics, University of Science and Technology of China, Hefei CN-230026, China

^dDepartment of Physics, Aristotle University of Thessaloniki, University Campus, GR-54124, Thessaloniki, Greece.

^eInstitute of Nuclear and Particle Physics, NCSR Demokritos, GR-15341 Agia Paraskevi, Attiki, Greece

^fNational Technical University of Athens, Athens, Greece

^gLaboratório de Instrumentação e Física Experimental de Partículas, Lisbon, Portugal

^hRD51 collaboration, European Organization for Nuclear Research (CERN), CH-1211 Genève 23, Switzerland

ⁱInstituto Galego de Física de Altas Enerxías (IGFAE), Universidade de Santiago de Compostela, Spain

^jLIDYL, CEA, CNRS, Université Paris-Saclay, F-91191 Gif-sur-Yvette, France

^kCEA-LIST, Diamond Sensors Laboratory, CEA Saclay, F-91191 Gif-sur-Yvette, France

¹Helsinki Institute of Physics, University of Helsinki, FI-00014 Helsinki, Finland

Abstract

This contribution describes the PICOSEC-Micromegas detector which achieves a time resolution below 25 ps. In this device the passage of a charged particle produces Cherenkov photons in a radiator, which then generate electrons in a photocathode and these photoelectrons enter a two-stage Micromegas with a

*Corresponding author (kordas@physics.auth.gr, kostaskordas@cern.ch)

¹Now at Synchrotron Soleil, BP 48, Saint-Aubin, 91192 Gif-sur-Yvette, France

²Also at National Research Nuclear University MEPhI, Kashirskoe Highway 31, Moscow, Russia and Department of Physics, Uludag University, TR-16059 Bursa, Turkey

³Also at University of Virginia, U.S.A

reduced drift region and a typical anode region. The results from single-channel prototypes (demonstrating a time resolution of 24 ps for minimum ionising particles, and 76 ps for single photoelectrons), the understanding of the detector in terms of detailed simulations and a phenomenological model, the issues of robustness and how they are tackled, and preliminary results from a multi-channel prototype are presented (demonstrating that a timing resolution similar to that of the single-channel device is feasible for all points across the area covered by a multi-channel device).

Keywords: Picosecond timing, MPGD, Micromegas, Photocathodes, Cherenkov radiators, Timing algorithms

1. Introduction and Detector Description

Particle detection with a time precision in the picosecond domain brings the field of High Energy Physics in the 4D tracking era. In the High Luminosity LHC, the high multiplicity (~ 140) of proton-proton interactions piling-up close to each other ($\sigma \sim 45$ mm) in the same proton-proton bunch crossing, will make the association of particles with the correct pp vertex a challenging task. Timing the arrival of particles with a resolution of the order of 30 ps can mitigate this problem [1]. For the needed large-area coverage and the high instantaneous and integrated particle fluxes seen in these experiments, Silicon and Micro Pattern Gaseous Detectors are good and relatively economic candidates, but they require significant modifications to reach the desired performance.

Recently, the RD-51 PICOSEC-Micromegas collaboration developed a technique [2] reaching below 25 ps [3]. In this device (Fig. 1) the passage of a particle produces Cherenkov photons in a radiator, which then generate electrons in a photocathode. These photoelectrons (p.e's from here on) enter a two-stage Micromegas [4] with a reduced drift region ($\sim 200 \mu\text{m}$) in order to minimize the possibility of ionisations by the passing particle, while the anode region has the typical size for Micromegas ($128 \mu\text{m}$). Thus, the p.e's are produced almost synchronously and they can start "preamplification" avalanches

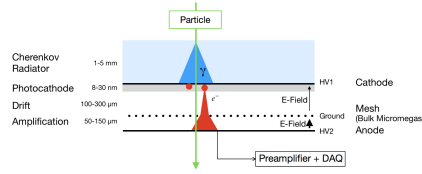


Figure 1: Layout of the PICOSEC-MicroMegas detector, described in the text.

20 (“pre-avalanches” from here on) early in the drift region with a small time jitter. Unless mentioned otherwise, results presented here are produced with the “nominal” detector, where the Cherenkov radiator is a 3 mm-thick MgF_2 layer, the photocathode is an 18 nm-thick CsI film deposited on a 5.5 nm-thick film of semitransparent Cr which provides conductivity to the cathode, the gas mixture is the “COMPASS” gas ($80\% \text{Ne} + 10\% \text{C}_2\text{H}_6 + 10\% \text{CF}_4$) at 1 bar, the drift
 25 region is $200 \mu\text{m}$ and the readout is a bulk Micromegas[5]. Single- and multi-pad devices were tested, as well as devices with different photocathodes and different resistive Micromegas readouts.

2. Response to single photoelectrons and to muons

30 The time response of a nominal single-pad (1 cm in diameter) PICOSEC-Micromegas detector to single p.e.’s and to MIPs (muons) was measured and reported in [3]. Fig. 2 shows a typical pulse caused by a muon and digitized by a 2.5 GHz oscilloscope every 50 ps. The fast component with a ~ 500 ps rise-time and a duration of ~ 1 ns is due to the current induced on the anode by the fast
 35 moving electrons and is called the “e-peak”. The slow component extending up to several hundred of ns is due to the slowly moving ions. The collected digitized waveforms were analysed offline to determine the e-peak start and end times, the e-peak charge and amplitude and the Signal Arrival Time (SAT), which is defined at 20% of the amplitude (i.e, using the Constant Fraction
 40 Discrimination, CFD, technique).

The time-reference-subtracted SAT distribution was fit to the sum of two Gaussians, whose weighted RMS yielded the resolution. The time reference was given with a precision of ~ 13 ps for single p.e.’s and ~ 5 ps for muons, by a photo

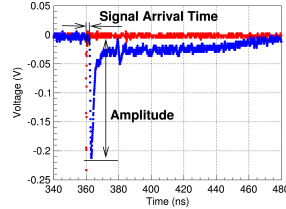


Figure 2: Example of a pulse produced by the PICOSEC-Micromegas detector responding to 150 GeV muons (blue), recorded together with the timing reference signal of a microchannel plate, MCP (red).

diode and by a microchannel plate (MCP), respectively. The time resolution
 45 improved with higher drift voltages, with a smaller dependence on the anode
 voltage. The best resolution for single p.e.'s was found to be (76.0 ± 0.4) ps, at
 an anode/drift voltage of +450 V / -425 V, respectively. For muons, the best
 resolution was (24.0 ± 0.3) ps, obtained with an anode/drift voltage of +275 V
 / -475 V, respectively.

50 The inadequacy of a single Gaussian to determine the resolution indicates
 that not all pulses have the same resolution. Indeed, in both the muon and the
 single p.e data, it was found (see Fig. 3, right) that the resolution improves
 as the e-peak charge increases, with the same dependence for all drift voltages.
 The SAT was also found (see Fig. 3, left) to vary with the e-peak charge,
 55 with the same power-law for all drift voltages, but shifted to lower levels for
 higher voltage settings. This shift reflects the increased electron drift velocity
 for higher drift voltages, but the dependence of the SAT on the e-peak charge
 is not evident. Since it was found that the pulse shape is identical for different
 e-peak charges, the use of the CFD technique should yield the same SAT for all
 60 pulses. Therefore, the observed SAT dependence on the e-peak charge must be
 caused by the physical mechanism generating the PICOSEC-Micromegas signal.

Muons generate multiple p.e.'s and thus bigger signals with improved reso-
 lution. The distribution of e-peak charges generated by single p.e.'s is described
 well by a Polya function (a Gamma distribution). For muons the distribution
 65 is also a Polya, which results from the convolution of the single p.e Polya and
 a Poisson describing the number of generated p.e.'s. The mean number of p.e.'s

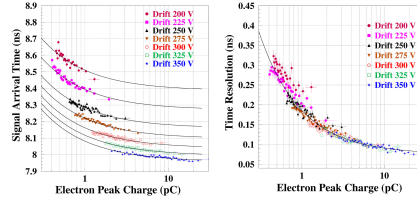


Figure 3: Mean SAT values (left) and time resolution (right) as a function of the e-peak charge, for single p.e data, for a fixed anode voltage of +525 V and drift voltages between -200 V and -350 V.

per muon is found to be 10.4 ± 0.4 for this nominal PICOSEC-Micromegas with a CsI photocathode.

3. Understanding the detector: simulation and modeling

In order to understand the origin of the SAT and resolution dependence on the e-peak charge, detailed simulations were performed, based on Garfield++ [6], where the response of the electronics to a single amplification avalanche is included [7]. Simulating up to the entrance of the pre-avalanche in the anode region and assuming a linear response of the electronics, the simulation produces waveforms, including a 2.5 mV RMS uncorrelated noise. The simulated pulses were digitized and analyzed in the same way as the real waveforms, and they exhibit exactly the same dependence of the SAT and the time-resolution on the e-peak charge as the real data seen in Fig. 3.

Investigating in detail, it was found [7] that there is a microscopic parameter with the same statistical properties (notably the mean and RMS) as the SAT, in every bin of the e-peak charge: this is the average arrival time of the preamplification electrons into the amplification region, having just traversed the mesh. The statistical properties of this microscopic variable are determined by the transmission time of the primary p.e from its emission from the photocathode until it causes the first ionisation, by the transmission time of the pre-avalanche to reach the mesh, and by the time needed to go through the mesh and enter the amplification region. The transmission time through the mesh is found to

be a constant. In contrast, both the p.e and the pre-avalanche mean transmission times increase linearly with distance, with the pre-avalanche having a
 90 higher effective drift velocity than the primary p.e ($154 \mu\text{m}/\text{ns}$ vs. $134 \mu\text{m}/\text{ns}$, respectively, for a drift/anode voltage of $-425 \text{ V} / +450 \text{ V}$).

A longer pre-avalanche means a shorter travel for the primary p.e. Thus, the difference in drift velocities means that, counting time from the emission of the primary p.e, the average total arrival time of the preamplification electrons on the mesh gets smaller for longer pre-avalanches. Since the transmitted
 95 fraction of electrons via the mesh is found to be constant and the amplification region gain is also a constant, the e-peak charge is proportional to the pre-avalanche electron population, which increases with the avalanche length. Thus, the smaller SAT values for larger e-peak charges are understood as a
 100 consequence of the pre-avalanche propagating faster than the primary p.e.

It was also found that the spread of the p.e's transmission time increases with larger drift paths, while the spread of the preamplification avalanche's transmission time is saturated at a constant value (see Fig. 4, left). Therefore, the sooner the primary p.e ionizes for the first time, the better the time
 105 resolution is. Notice though that the spread of the total transmission time is smaller than the quadrature sum of the time spreads of the primary p.e and the pre-avalanche, indicating that the p.e and avalanche transmission times are heavily correlated. (Since longer pre-avalanches produce on average larger e-peak charges, the spread of the transmission times gets smaller as the number
 110 of pre-avalanche electrons increases (see Fig. 4, right).

In order to gain insight on the main physical mechanisms causing the findings mentioned above, a phenomenological model was built [8]. Motivated by the known fact in the literature that quenchers in the gas-mix increase the drift velocity, the model is based on a simple mechanism of "time-gain per inelastic
 115 interaction" compared to an elastic interaction and it employs a statistical description of the avalanche evolution, taking into account all correlations between the various players. The model describes the dynamical and statistical properties of the microscopic quantities determining the PICOSEC-Micromegas

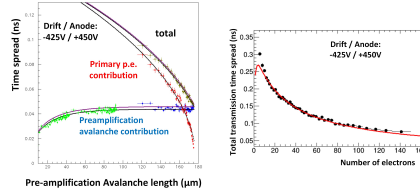


Figure 4: Left: spread of transmission times vs. pre-avalanche length (a long pre-avalanche means a short p.e path), for: i) the primary p.e before it ionizes for the first time (red points), ii) the pre-avalanche from its initiation until the mesh (blue points; green points correspond to avalanches which have not yet reached the mesh) and iii) the total transmission time from the creation of the primary p.e's to the arrival of the pre-avalanche to the mesh (black points). Right: the spread of the total transmission time vs. the number of electrons reaching the mesh. All results are from detailed Garfield+++ simulations with anode and drift voltages of +450 V and -425 V, respectively. The lines are not fits to the data, but predictions of the model (see text).

timing characteristics, in an excellent agreement with the detailed simulations
 120 (see lines in Fig. 4). Since it uses complete PDFs in its equations, it does not
 only describe mean and RMS values, but full distributions as well. In paral-
 lel, it offers phenomenological explanations to the behavior of the microscopic
 variables (e.g., the faster drifting of the pre-avalanche compared to the primary
 p.e, the saturation of the time spread of the pre-avalanche's electrons, etc.).
 125 The model can be used as a tool for fast and reliable predictions, provided the
 values of the model input-parameters (e.g. drift velocities) are known. Having
 available sets of input parameter values for certain operational settings, empir-
 ical parameterizations are derived, which can be used to provide the values of
 the input parameters to the model for the whole region of operational settings
 130 covered by the above parameterizations [8].

4. Towards a robust and large scale device

4.1. Robustness issues

It was shown above that the best timing resolution is achieved for large
 e-peak charges. These are achieved with high electric fields, but the voltages
 135 cannot take arbitrary values: e.g., for the case of the beam test with muons,

at a drift voltage of -475 V, the maximum anode voltage for which there were no discharges during the beam run, was $+275$ V. But, for a detector to operate efficiently at high particle fluxes, it has to be robust against sparks (discharges). With all other things kept the same as for the nominal PICOSEC-Micromegas, two different resistive PICOSEC-Micromegas designs have been successfully tested to mitigate such problems. One uses a resistive material layer on top of the anode [9] and the other uses a conductive copper layer coupled to ground by a resistor (referred to as a “floating strip” Micromegas [10]). Different resistive layers (0.3 - 10 M Ω /square), as well as a floating strip prototype with a 25 M Ω coupling has been operated stably at a high rate pion beam. Trying various voltage settings, the best *preliminary results* for the timing resolution were $\sim 35 - 40$ ps for the resistive Micromegas setups, and ~ 30 ps for the floating strip setup.

After the heavy irradiation tests above though, it was seen with the microscope that the CsI photocathode was damaged. Such damage can be caused by Ion Back-Flow, where ions created along with the electrons during the avalanche development are flowing back towards the cathode. Exposure of the photocathode to humidity in air, which can happen depending on the storage conditions, can also damage the photocathode and deteriorate its performance. A photocathode should also have a relatively high quantum efficiency, in order to get a reasonable number of p.e.’s per passing muon. In fact, the time resolution is proportional to the inverse of the square of the number of p.e.’s; as seen in Section 2 for the nominal device, the resolution for the single p.e. case is about $\sqrt{10.4}$ times bigger than the resolution for the muon case (76 ps vs. 24 ps, respectively). Various photocathodes were tested with these requirements in mind; from metallic (e.g., Al), to CsI with thicker Cr layers than the nominal 5.5 nm, to Diamond-Like Carbon (DLC) films. *Preliminary results* show that a 2.5 nm DLC film is promising, being robust against long storage periods and yielding around 3.7 p.e.’s per muon, reaching a resolution down to $\sim 35 - 40$ ps. More results can be found at [11].

4.2. Response of a multi-pad device to muons

On the way towards large-scale PICOSEC-Micromegas devices, a multi-pad prototype has been constructed and tested in muon beam. All characteristics where like in the nominal detector configuration, but the anode was segmented in 5 mm-side hexagonal pads and four of them were read out in a setup identical
 170 to the single-pad case, but using two oscilloscopes.

The response of each pad vs. the distance R of the track impact point from the pad center, was studied. The average e-peak charge will decrease as the distance R increases, but the e-peak charge value incorporates the information
 175 about where is the Cherenkov cone centered compared to the pad center. So, universal curves vs. e-peak charge should be observed for events with different R values. This was not the case due to some geometrical distortion of the chamber which resulted in a different response as a function of R and ϕ around each pad's center. After correcting the observed SAT values for these effects,
 180 universal curves were obtained for the SAT and time resolution vs. e-peak charge; one pair of such curves for each pad.

Following the same analysis steps as for the single-pad prototype, each pad was found to have a *preliminary time resolution* of ~ 25 ps, for tracks passing within 2 mm from its center. In the region between three pads the distance from
 185 each pad-center is maximum and each individual pad sees a smaller average e-peak charge; thus, each pad alone exhibits a resolution with *preliminary values* in the range $\sim 70 - 80$ ps. A naive combination of these individual-pad results would yield a time resolution around 45 ps for such tracks. But, since the expected SAT and time resolution of each event in each pad is known from
 190 the corresponding curves vs. the e-peak charge in each pad, a combined event-by-event measurement of the SAT can be obtained. The resolution of the SAT distribution is found to have the *preliminary value* of ~ 30 ps, which is close to the value obtained when the track goes through the center of each pad. Confidence to this result is obtained by observing that the pull-distribution of the SAT
 195 values is a normal Gaussian, with a mean and sigma value consistent with zero and one, respectively. Similar time resolution was observed all across the area

covered by the four pads, proving that a multi-pad detector can yield a time resolution comparable to a single-pad device.

5. Conclusion

200 The progress towards a well understood, robust, large-area, PICOSEC-Micromegas detector offering precise timing in the HL-LHC era and beyond was presented in this work. Single-channel prototypes have demonstrated an excellent time resolution, of (76.0 ± 0.4) ps for timing a single photoelectron and (24.0 ± 0.3) ps for timing the arrival of a MIP, using a CsI photocathode which
205 yields on average 10.4 ± 0.4 photoelectrons per MIP. The PICOSEC-Micromegas timing characteristics have been extensively studied in terms of detailed simulations and understood in detail in terms of a phenomenological model. Working towards a robust device, tests with resistive anode configurations were performed, demonstrating tolerance to high particle fluxes but a somewhat worse
210 time resolution. Various photocathodes were also tested for their robustness against Ion Back Flow and storage conditions, as well as their quantum efficiency with promising results. Last, a multi-pad PICOSEC-Micromegas device was constructed and tested in muon beam and preliminary results show that the timing resolution is better than about 30 ps all across the area covered by
215 the device.

Acknowledgments

We acknowledge the financial support of the Cross-Disciplinary Program on Instrumentation and Detection of CEA, the French Alternative Energies and Atomic Energy Commission; the RD51 collaboration, in the framework of
220 RD51 common projects; and the Fundamental Research Funds for the Central Universities of China. L. Sohl acknowledges the support of the PHENIX Doctoral School Program of Université Paris-Saclay. J. Bortfeldt acknowledges the support from the COFUND-FP-CERN-2014 program (grant number 665779). M. Gallinaro acknowledges the support from the Fundação para a

225 Ciência e a Tecnologia (FCT), Portugal (grants IF/00410/2012 and CERN/FIS-
PAR/0006/2017). D. González-Díaz acknowledges the support from MINECO
(Spain) under the Ramon y Cajal program (contract RYC-2015-18820). F.J.
Iguaz acknowledges the support from the Enhanced Eurotalents program (PCOFUND-
GA-2013-600382). S. White acknowledges partial support through the US CMS
230 program under DOE contract No. DE-AC02-07CH11359.

References

- [1] S. White, Experimental challenges of the European Strategy for particle physics, in: Procs, Int. Conf. on Calorimetry for the High Energy Frontier (CHEF 2013) Paris, France (2013) April 22–25,
235 http://inspirehep.net/record/1256027/files/CHEF2013_Sebastian.White.pdf.
- [2] T. Papaevangelou, et al., Fast Timing for High-Rate Environments with Micromegas, In EPJ Web of Conferences. 4th Int. Conf. on Micro Pattern Gaseous Detectors (MPGD 2015) 174.
- [3] J. Bortfeldt, et al., Picosec: Charged particle timing at sub-25 picosecond
240 precision with a micromegas based detector, Nucl. Instrum. Meth. A 903 (2018) 317–325.
- [4] Y. Giomataris, P. Rebourgeard, J. P. Robert, G. Charpak, A High granularity position sensitive gaseous detector for high particle flux environments, Nucl. Instrum. Methods A 376 (1996) 29–35.
- 245 [5] I. Giomataris, et al., Micromegas in a bulk, Nucl. Instrum. Meth. A 560 (2006) 405–408.
- [6] H. Schindler, R. Veenhof, Garfield++ simulation of tracking detectors, <https://garfieldpp.web.cern.ch/garfieldpp/>.
- [7] K. Paraschou, Study of the PICOSEC Micromegas Detector with Test
250 Beam Data and Phenomenological Modelling of its Response, Mas-

ter's thesis, School of Physics, Aristotle University of Thessaloniki,
<https://ikee.lib.auth.gr/record/297707/> (2018).

[8] J. Bortfeldt, et al., Modeling the Timing Characteristics of the PICOSEC
Micromegas Detector (2019), arXiv:1901.10779v1 [physics.ins-det].

255 [9] T. Alexopoulos, et al., A spark-resistant bulk-micromegas chamber for
high-rate applications, Nucl. Instrum. Meth. A 640 (2011) 110–118.

[10] J. Bortfeldt, The Floating Strip Micromegas Detector, Springer, 2015.

[11] L. Sohl, et al., Picosec-Micromegas: Robustness measurements and study of
different photocathode materials, J. Phys.: Conf. Ser. **1312** 012012 (2019).
260 Proceedings in 9th Symposium on Large TPCs for Low-Energy Rare Event
Detection, Paris, France, Dec. 2018.